

INTERNATIONAL SOCIETY FOR SOIL MECHANICS AND GEOTECHNICAL ENGINEERING



This paper was downloaded from the Online Library of the International Society for Soil Mechanics and Geotechnical Engineering (ISSMGE). The library is available here:

<https://www.issmge.org/publications/online-library>

This is an open-access database that archives thousands of papers published under the Auspices of the ISSMGE and maintained by the Innovation and Development Committee of ISSMGE.

Geostatistical comparison of geotechnical properties; Orphan Basin, St. Pierre and Scotian Slopes



Valerie Latour, *Mitchelmore Engineering, Nova Scotia, Canada*
Kevin MacKillop, *GSC (Atlantic), Nova Scotia, Canada*
Perry Mitchelmore, *Mitchelmore Engineering, Nova Scotia, Canada*
Dave Mosher, *GSC (Atlantic), Nova Scotia, Canada*

ABSTRACT

Oil and gas exploration in Eastern Canada has included deep water regions of the Orphan Basin, St. Pierre slope and Scotian slope. The Geological Survey of Canada, in collaboration with non-government agencies, has undertaken a program to understand deep water margin geologic processes and potential geohazards. Short (<10 m) piston cores have been analysed to assess the geology, geotechnical properties, stress history, and static failure potential. Material properties for density, composite lab minivane and shipboard torvane undrained shear strength are assessed using random field theory to characterize the three regions separately. A slope stability analysis of near surface sediments was evaluated using the infinite slope method to assess the probability of slope failure for each region using a total stress analysis. This paper compares the three regions for common and anomalous characteristics and trends.

RÉSUMÉ

Les explorations pétrolières dans l'Est du Canada se sont étendues aux régions hauturières du Bassin d'Orphan, des pentes de St Pierre et de la Nouvelle-Ecosse. La Commission Géologique du Canada, en collaboration avec des agences non gouvernementales, a engagé un projet d'étude sur la compréhension des processus géologiques en domaine océanique profond et les risques potentiels associés. De courtes carottes (<10 m) ont été analysées afin d'en déterminer la géologie, les propriétés géotechniques, l'histoire des contraintes, et le potentiel de rupture statique. Les propriétés matérielles pour la densité, les mesures non drainées des forces de cisaillements sur des échantillons minivan de laboratoire et torvane prélevés à bord du navire, sont déterminées en utilisant des champs théoriques aléatoires pour caractériser séparément les trois régions. Une analyse de stabilité de pente à proximité des sédiments de surface a été effectuée à contrainte totale en utilisant la méthode de la pente infinie afin d'évaluer la probabilité de rupture de pente pour chaque région. Cet article compare les caractéristiques communes, les anomalies et les tendances de ces trois régions.

1 INTRODUCTION

The objective of this study is to conduct a geohazard assessment of the Central Scotian slope, St. Pierre slope and Orphan Basin (Figure 1) with an emphasis on regional slope stability risk and critical slope inclinations. This comparative geohazard assessment was conducted using available geotechnical data obtained short piston core (<10 m) piston cores.

The assessment is developed using two separate but interconnected models, the geotechnical model and the engineering model. The geotechnical model is developed by assessing the available geotechnical data obtained from the GSC-A core processing lab, compiling and assigning strength parameters, index parameters and physical parameters. Meco contributed to the process by synthesizing and assimilating data, organizing and processing data and by providing a process to incorporate the data into the engineering model. The engineering model is developed to consider possible loading conditions and predict the soil resistance to these conditions. The current model considers total stress analysis using the infinite slope model for slope stability. In addition to developing the

project in all aspects previously explored by Meco (2008), the current study had three overriding requirements: 1) Process additional geotechnical data to the same level as the previous Scotian Slope study (Meco 2007) and then review core data sets for all three regions; 2) Assess the probability of slope failure for the region using the methodology developed in the previous study (Meco 2007) for the infinite slope method and total stress analysis and 3) Compare the three regions, for common and anomalous characteristics and trends.

2 GEOLOGICAL SETTING

2.1 Scotian Slope

The geological setting of the Scotian Shelf has been established by others and was not re-interpreted in this work. A synopsis again presented below.

Generally, the Scotian Shelf is part of the Mesozoic rifted margin of the central North Atlantic Ocean, with thick Jurassic and Cretaceous strata overlying Triassic salt (Wade and Maclean, 1990). The upper few hundred metres of the sedimentary sequence beneath the Scotian

slope consist of a thick progradational Tertiary succession, overlain both conformably and unconformably by Quaternary sediments. Deposition of near surface sediments was controlled by glacial processes. The first shelf-crossing glaciation event occurred about 0.5 Ma and since that time, the continental slope has been dominated by proglacial sediment deposition, with little sediment accumulation at high-stands.

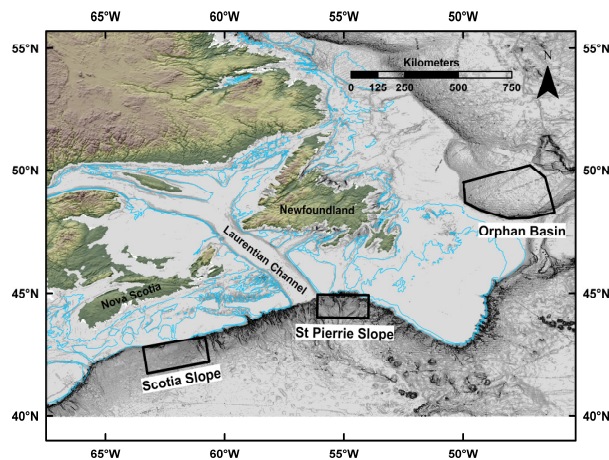


Figure 1. Location of study areas

The relative sea level through geological history will have varied from the present level. The Holocene (past 10,000 years) is believed to be a period of transgression and relatively light, hemiphalagic deposition. Regression periods during the late and middle Pleistocene, where relative sea levels may have been 110 to 120 m below present, are believed to be periods of more active deposition.

The present near surface sediment in the study area is understood to be transported glacial moraine, deposited either hemiphalagically or by mass transport and debris flows. The cause of mass transport is not well understood but earthquakes are generally thought to be a factor (e.g. 1929 Grand Bank earthquake). In this slope environment, ground-shaking can remobilize sediment and cause massive landslides as it did in the 1929 event (Piper and Normark, 1982).

There is little evidence of sediment failures in the last 10 ka and slope stability analysis has shown the surface sediment to be statically stable, except on steep escarpments and canyon walls. There is, however, abundant evidence of sediment failures that approximately correlate to glacial advances (25-12 ka, ~75 ka, ~130 ka) suggesting a potential loading situation likely to cause failure (Mosher et al. 1994).

2.2 Orphan Basin

The geological setting of the Orphan Basin is described in the Geological Survey of Canada Open File 5299 (Tripsanas et al. 2007) and is summarized below.

The Orphan Basin is located northeast of Newfoundland and is characterized as a natural glaciomarine laboratory with a highly variable sedimentological regime. The Orphan Basin can be divided into seven discrete geomorphic areas, each dominated by different sedimentary processes: Orphan Spur, Sackville Spur, Trinity Trough Fan, Sheridan Canyon, Bonanza Canyon and Sackville Canyon.

The Orphan and Sackville Spur areas are affected by deposition from meltwater plumes which have been redirected by bottom currents. The Labrador Current is the major agent for the redirection of the meltwater plumes. The plume deposits are characterized as carbonate-rich and chocolate-red stratified clayey mud deposits. The carbonate-rich deposits originated from Hudson Bay during catastrophic melt water plumes with periodicity of around 7000 years. The chocolate-red stratified clayey mud deposits, which are interbedded with 0.5 cm to several centimeter thick layers of ice rafted debris layers, originated from St. Anthony Basin of the northeast Newfoundland Shelf.

The Trinity Trough Fan area consists of successive and widespread pockets of mounded, glaciogenic debris flows which occurred during glacial periods. The Sheridan and Bonanza Canyons are characterized by high (~100 m to ~700 m) and rough relief. Canyons have resulted from retrogressive sediment failures that have punctured well into the till deposits on the upper slope and outer shelf. The Sackville Canyon consists of a larger number of low relief (~50 m to ~150 m) gullies separated by well-stratified overbank areas. Morphology attributed to plume deposition channels represent gravity flows originating from a glacier that did not advance to the shelf edge. The Sheridan Canyon system formed directly above the glaciogenic debris-flow deposits of the Trinity Trough Fan and is therefore immature and lacks well developed levees. The Bonanza and Sackville Canyon systems are characterized by well-developed levees with some mud waves (Tripsanas et al. 2007).

2.3 St. Pierre Slope

The St. Pierre slope is a broad, relatively flat area bounded on the east and west by canyons. The lower slope is cut by four box-shaped valleys that are several kilometres wide and approximately 200 m deep. The mid-slope has a terraced morphology with several sinuous escarpments, ranging from 2 m to over 100 m in height, across it. Between 500 and 2000 metres water depth the predominant morphological features are the sinuous escarpments which are presumably formed by retrogressive failure. Between 2000 m and 2500 m water depth the slope is steeper and is incised by a series of 100 m to 150 m deep sub-parallel gullies with few tributaries. These gullies resemble valleys on the Scotian slope which have been interpreted as retrogressive headwall failure. Failures in the St. Pierre slope area have been interpreted as wide spread (Moser and Piper, 2007).

3 GEOTECHNICAL MODEL

The study considers three separate regions. The Scotian slope of Nova Scotia, the St. Pierre slope and Orphan Basin of Newfoundland and Labrador. The geotechnical model developed for each region is dependent on physically measured characteristics and does not consider lithostratigraphy or biostratigraphy.

3.1 Available Data

The Scotia slope study region measures approximately 175 km east-west by 75 km north-south. The analysis includes geotechnical data from 57 sites. The total sample frequency is approximately 3.9 sites per 1000 km². The St. Pierre slope study region measures approximately 300 km east-west by 80 km north-south and includes 21 sites for a sampling frequency of approximately 0.92 sites per 1000 km². The Orphan basin study region measures approximately 400 km east-west by 285 km north-south and includes 46 sites for a sampling frequency of approximately 0.77 sites per 1000 km².

The seabed inclination at each core location was obtained from multibeam bathymetric surveys completed for each study region and are summarized in Table 1. The seabed inclination for the core sites varied from 1.0° to 10.7° for the Scotian slope, 0.5° and 19.5° for St. Pierre slope and 0.1° and 11.0° for Orphan Basin. The data reveals that Orphan Basin is less steep on average, followed by the Scotia slope and St. Pierre slope study regions.

Table 1. Measured Seabed Angles

| | Scotian Slope | Orphan Basin | St. Pierre Slope |
|---------|---------------|--------------|------------------|
| Mean | 3.4 | 1.2 | 5.1 |
| Minimum | 1.0 | 0.1 | 0.5 |
| Maximum | 10.7 | 11.0 | 19.5 |

Cores were collected from the seabed using the Long Corer Facility (LCF). The device collects a 100 mm diameter, 7 m to 15 m long relatively undisturbed sediment core. Trigger weight and piston cores were typically recovered at each site. The trigger weight core can be used to account for surface sediment not recovered in the piston core. The trigger weight and piston core data were integrated to construct a composite data set for each site.

Core processing was done on both piston and trigger weight cores at the GSC-A core processing laboratory. The core is initially processed in the Multi Sensor Track logger (MST). The MST measures bulk density, magnetic susceptibility and compressional wave velocity at 1 cm intervals. The core is then split with one half designated as the archive and one half as the working half. The archive half was digitally photographed and visually described. Discrete index property samples, laboratory

miniature vane shear strength and acoustic velocity measurements were taken at 10 cm intervals on the working half. The undrained shear strength measurements were made using an automated miniature laboratory vane apparatus. Measurements were not made at intervals where drained conditions existed (sandy sediments) or on sediment containing numerous clasts.

3.2 Physical Characteristics

The test data for each core was assessed for use in the engineering model. Descriptive statistics and plot profiles for bulk density and undrained shear strength indicate the measured shear strength has a positive mean trend and relatively constant variance with depth while the measured bulk density is relatively constant in mean and variance with depth.

The trend is likely to be a function of the stress domain of the lithostratigraphic units (i.e., preconsolidation pressure) but there was insufficient data to segregate soil units in the vertical direction. Qualitatively, the trend in bulk density is expected to be unique and independent of depth for each lithostratigraphic soil unit, whereas, for undrained shear strength, it is expected to be linearly increasing with depth. Since all data were measured in the vertical dimension, values can be expressed as a function of depth by:

$$S_u(z)=a+bz+\epsilon(z) \quad [1]$$

where S_u is the undrained shear strength, b is the trend of S_u with depth, a is the mean of S_u at surface ($z=0$) and $\epsilon(z)$ is the random error. The random error term is a measure of uncertainty in sampling and measurement. If the trend is an unbiased estimate of the mean undrained shear strength at depth z , then the random error $\epsilon(z)$ will have zero mean.

A systematic assessment of each core section was performed to investigate suspect low and high shear strength measurements. The objective of the assessment was to remove data measurements that are anomalous and potentially misleading. Individual cores with a mean bulk density that is not within 3 standard deviations of the mean for its respective region were removed from the data set. Individual cores with a mean de-trended shear strength that is not within 3 standard deviations of the mean for their respective region were also removed from the data set.

The descriptive statistics for bulk density values for each region are presented in Table 2. The data was not filtered or transformed to remove trends or to segregate different strata. The descriptive statistics for the undrained shear strength values for each region are presented in Table 3.

Table 2. Descriptive Statistics for Bulk Density (g/cm³)

| | Scotian Slope | Orphan Basin | St. Pierre Slope |
|------------------------------|---------------|--------------|------------------|
| Mean | 1.69 | 1.87 | 1.66 |
| Minimum | 0.47 | 1.32 | 1.33 |
| Maximum | 3.67 | 2.38 | 1.99 |
| Standard Deviation | 0.14 | 0.17 | 0.11 |
| Coefficient of Variation (%) | 8.20 | 9.16 | 6.55 |

Table 3. Descriptive Statistics for Undrained Shear Strength (kPa).

| | Scotian Slope | Orphan Basin | St. Pierre Slope |
|------------------------------|---------------|--------------|------------------|
| Mean | 10.1 | 11.2 | 11.2 |
| Minimum | 0.5 | 2.7 | 2.6 |
| Maximum | 93.3 | 26.2 | 23.1 |
| Standard Deviation | 6.6 | 5.8 | 4.6 |
| Coefficient of Variation (%) | 65.0 | 50.4 | 40.9 |

3.3 Data Processing

The undrained shear strength data tended to increase linearly with depth. Prior to performing statistical analysis, the undrained shear strength needed to have the trend removed. To accomplish this, for each core in each region, the undrained shear strength of the i 'th core, S_{ui} , was fit with a straight line according to:

$$\hat{S}_{u1} = a_1 + b_1 z, \hat{S}_{u2} = a_2 + b_2 z, \dots, \hat{S}_{un_c} = a_{n_c} + b_{n_c} z \quad [2]$$

where n_c is the total number of cores, z is the depth below the seabed and a_i and b_i are the intercept and slope, respectively, for the regression line. The regression tool in MS Excel was used to determine a_i and b_i for all core datasets.

In the case of local de-trending, for each individual core, the regression for undrained shear strength as a function of depth was transformed in order to estimate shear strength independent of depth.

For the regional analysis, core datasets were combined for each region and a regression line was fit to the aggregate data. The average trend, \hat{S}_u was estimated from a regression of the aggregate dataset with intercept and slope, \bar{a} and \bar{b} . The average trend, \hat{S}_u , was removed from all core data to produce a 'detrended' data set for each core. The detrended data at depth $z_j = (j-1)\Delta z$, where Δz is the depth increment between observations, along the i 'th core will be referred to as T_{ij} , where

$$T_{ij} = S_{ui}(z_j) - (\bar{a} + \bar{b}z_j) \quad [3]$$

The detrended data sets were only used to identify outlier cores in this study.

4 ENGINEERING MODEL

The current scope of this study required analysis of slope stability similar to previous analysis performed for the Scotian slope (Meco 2007). This analysis was restricted to near surface sediments using a total stress analysis with undrained shear strength and bulk density measured from seabed to total depth of sampling.

4.1 Slope Stability Model

Slope stability is generally estimated using limit equilibrium methods and expressed as a factor of safety with respect to failure in the following form.

$$Factor\ of\ Safety = \frac{Available\ Shear\ Strength}{Equilibrium\ Shear\ Strength} \quad [4]$$

The factor of safety (FOS) is calculated using the equations of static equilibrium applied to a soil mass bounded by an assumed potential slip surface and the surface of the slope itself. For any defined system, the number of unknowns are greater than the number of equations and solving the equations requires simplifications and assumptions. To complete the analysis, in terms of the number of slices, n , the number of unknowns for static equilibrium analysis equals $5n-2$ while the number of equations is $3n$. In other words, only in the case of one slice is equilibrium statically deterministic. This one slice analysis method is known as the infinite slope method and represents a lower bound or a worst case scenario estimate of slope stability.

A total stress analysis (TSA) is performed assuming an undrained in-situ condition. The factor of safety is defined by:

$$FS = \frac{S_u}{\gamma_B z \sin \alpha \cos \alpha} \quad [5]$$

where S_u is the peak undrained shear strength of the soil, α is the slope inclination, γ_B is the buoyant unit weight of the soil above the potential failure plane and z is the vertical distance from the potential failure plane to the

surface. Discrete values for each parameter are entered into the equation to estimate the FS at depth z.

4.2 Probabilistic Method

The probabilistic assessment is performed using a Taylor series approximation of Equation 6 based on moments of the random variable of undrained shear strength. The Taylor series is expanded about the mean of the undrained shear strength and the series is truncated at the linear term. The FOS method only considers first order (i.e., linear) terms of the series. The seabed inclination and the bulk density of the sediments are assumed deterministic and the mean, or expected value, of factor of safety is estimated by:

$$E[FS] = FS \left[E[S_u] * \left(\frac{1}{\gamma H} \right) \right] \frac{1}{\cos \alpha \sin \alpha}$$

[6]

The variance of the factor of safety is expressed by:

$$VAR[FS] = \sum \left[E \left(\frac{\partial FS}{\partial S_u} \right)^2 VAR(S_u) \right]$$

[7]

where the partial derivative is taken at the mean in this instance. The derivatives are estimated numerically by evaluating the function at two points, one above and one below the mean.

If a lognormal distribution of FS of a sample set is assumed, (as is often the case with factor of safety distribution) then the expected FS value is the natural log of the expected FS value. Also the distribution of the standard deviation of the natural logarithms is a function of the coefficient of variation of the random variables. Again assuming a logarithmic distribution of FS, the 75 percentile and 90 percentile FS estimates can be determined in a fairly straightforward manner.

4.3 Local Analysis

A semiprobabilistic engineering model is used to assess the factor of safety for each core sample. The FOSM method was applied to each depth for all cores by considering undrained shear strength as a random variable while all other parameters were deterministic. Three estimates of factor of safety are calculated for each depth interval. One estimate is at the mean undrained shear strength and one estimate each at \pm one standard deviation of the mean.

Assuming a lognormal distribution for the factor of safety, the variance for factor of safety can be calculated. A distribution can also be estimated based on the range for that depth interval. The 50 percentile (median), 75

percentile and 90 percentile values for factor of safety are calculated for each depth from the estimated distribution. The result is a vertical profile of factor of safety with depth for each core.

The vertical profile, as can be seen in Figure 2, reveals that factor of safety decreases with depth. The decrease is rapid for shallow depths but becomes less rapid with increasing depth. This diminishing decrease is predicted by the function definition (Equation 6) which reduces to the inverse of the depth when all other variables are held constant.

The infinite slope method is a simplification; therefore certain limiting criteria were needed to select an appropriate factor of safety with depth for each core. The two available alternatives were, 1) select a value at a pre-determined depth or 2) select a tolerance value where by differences in factor of safety are thought inconsequential. The latter method was used for selecting factor of safety for each core using an arbitrary 2% as the

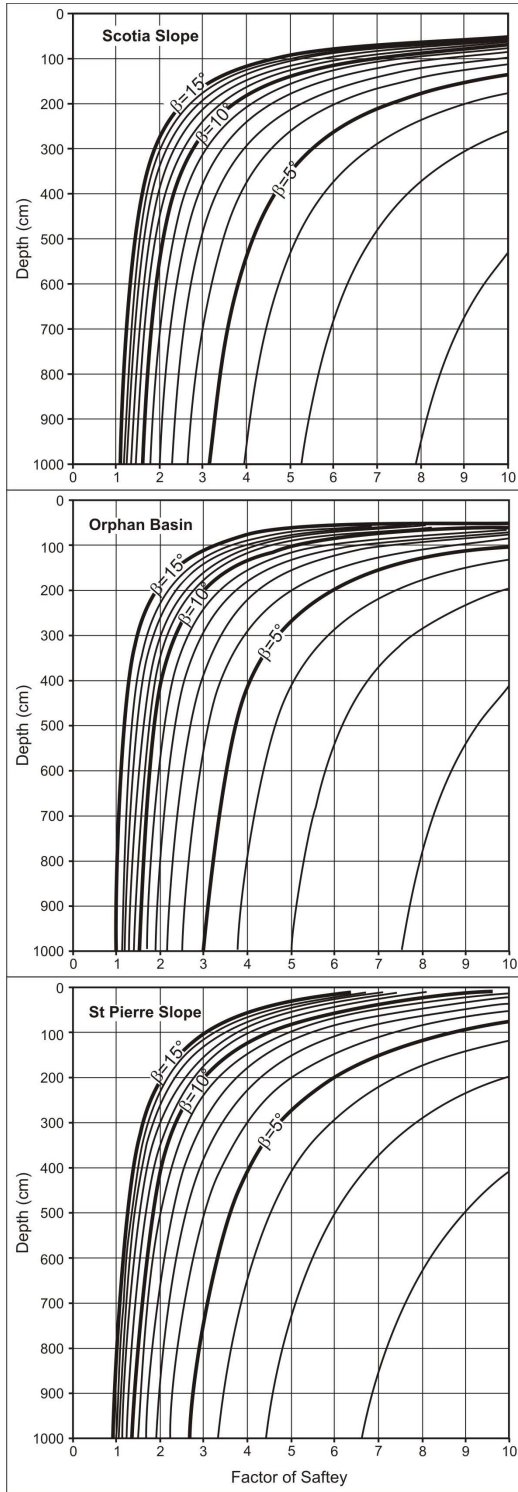


Figure 2. Factor of safety as a function of depth below seabed surface and seabed angle (β) for each region.

limiting criterion. The critical depths, defined as the depth at which the limiting criteria was established, are presented in Table 5. Other limiting criteria would have

adjusted the depths slightly, but these values were near the lower end of the inflection point of the curve and appear reasonable.

Table 5. Descriptive Statistics for Critical Depth (metres below seabed)

| | Scotian Slope | Orphan Basin | St. Pierre Slope |
|---------|---------------|--------------|------------------|
| Mean | 5.5 | 3.4 | 6.1 |
| Minimum | 1.9 | 0.3 | 3.0 |
| Maximum | 9.9 | 9.5 | 12.3 |

The factors of safety with the 50%, 75% and 90% probability of exceedance are plotted in percentile form in Figure 3. The most conservative assessment criteria of ninety percentile reveals that for each region there is a nominal risk of a factor of safety less than unity. The risk increases from 3% at Orphan Basin to 10% at Scotian slope to 18% at St. Pierre slope. For the least conservative assessment criteria of fifty percentile, only the St. Pierre (2%) study region has a nominal risk of factor of safety less than unity. At seventy five percentile, which is a reasonably conservative estimator (Meyerhof 1985), Scotian slope (2%) and St. Pierre slope (2%) have nominal risk of a factor of safety less than unity.

4.4 Global Analysis

Global trends of both undrained shear strength and effective overburden pressure were estimated. The global trends with depth were estimated from a regression of the aggregate data set as described in section 3.3. Using the data trends for undrained shear strength and effective overburden pressure and assuming the seabed inclination to be deterministic, the global trend of factor of safety with depth is estimated using Equation 6.

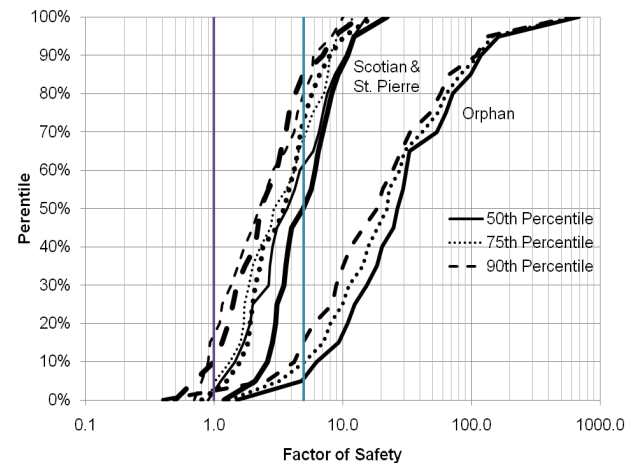


Figure 3. The factors of safety with 50%, 75% and 90% probability of expedience.

4.5 Reliability Assessment

The reliability of the analysis is a function of the probability that the factor of safety will be less than unity. Reliability should be understood as relative reliability, and not a measure of true reliability. The actual reliability is a function of the methodology adopted. The infinite slope method is a gross simplification of actual stress fields and tends to provide conservative estimates. Also, the method used to assess undrained shear strength will tend to underestimate the actual field value. These conservative assumptions are offset when using the total stress analysis, which is applicable to a limited number of loading cases and tends to be unconservative for other loading cases.

The reliability index is a measure of the risk at a site. It is determined as the number of standard deviations the average factor of safety value is from the defined failure criteria for the distribution of factor of safety. The reliability index defined using a factor of safety of unity for the failure criteria was found for each sample site and is presented by study region in Table 6.

Table 6. Descriptive Statistics for Reliability Index

| | Scotian Slope | Orphan Basin | St. Pierre Slope |
|---------|---------------|--------------|------------------|
| Mean | 7.1 | 19.7 | 3.8 |
| Minimum | 0.3 | 0.9 | 0.4 |
| Maximum | 117.0 | 153.8 | 13.3 |

The results describe all regions as stable and reliable. However, if the reliability index is plotted with the corresponding fifty percentile factor of safety (Figure 4), it is obvious that the failure criteria of the factor of safety at unity is inappropriate for the methodology used (i.e., total stress analysis using the infinite slope method). A target reliability index of 2.5 was selected for offshore structures, which is consistent with an expected 30 year life designed for a 100 year return event. Due to the variability of the data, a factor of safety of 5 seems to be more appropriate if reliability is the governing criteria.

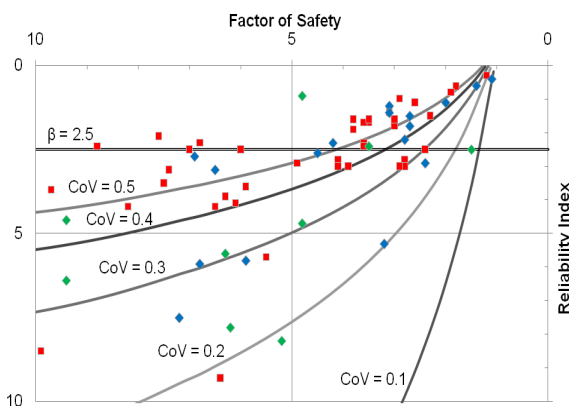


Figure 4. Reliability index and factor of safety fifty percentile

5 DISCUSSION AND FINDINGS

Analysis of slope stability was performed using the infinite slope method for the Scotian slope, the St. Pierre slope and the Orphan Basin. Each region was sampled to shallow depths (<10 m) using the GSC-A Long Corer Facility (LCF). There are 51, 21 and 50 sites available for the Scotia slope, St. Pierre slope and Orphan Basin study regions, respectively.

Data for each region was provided by GSC-A and included sample location, water depth, seabed inclination, bulk density and undrained shear strength. Descriptive statistics were used to assess average values and variance of data for each region. Generally speaking, the Orphan region sample sites are more uniform with respect to seabed inclination with an average inclination of approximately 1°. The Scotian slope and St. Pierre slope regions have similar average seabed inclinations in the range of 3° to 5°, respectively. The St. Pierre slope has the greatest range in seabed inclination between the sample sites.

Physically, the Orphan region has an average bulk density approximately 10% higher than either the Scotian slope or St. Pierre slope. The undrained shear strength comparison did not suggest any significant difference between regions in terms of descriptive statistics. However, there is considerable variability in the undrained shear strength data with a coefficient of variation varying from 40% to 65%. This variability is related to the trend in undrained shear strength, which is typically linear with depth.

Data for undrained shear strength was modified to remove the trend with depth to permit statistical analysis for a probabilistic engineering assessment. Two methods of de-trending were employed to accommodate the local and regional assessment modes. The local de-trending method included a regression assessment of trend with depth and the removal of the trend by subtracting the mean trend from the point values. This allows for a plot of undrained shear strength, with a constant mean value, with depth but maintaining the variance of the data. The regional de-trending included a regression assessment of all sample locations in each region, calculation of an average trend and then removal of the average trend for each sample core. This allows for a plot of undrained shear strength with depth as per the regional frame of reference. The de-trended data was used to assess variance of the physical parameters for engineering analysis. In the local model, undrained shear strength was modeled as a random variable while all other physical parameters, seabed inclination and bulk density were modeled as deterministic. In the regional model, undrained shear strength and bulk density were considered as random variables and seabed was taken as deterministic.

The engineering model uses the infinite slope method of slope stability analysis in a probabilistic framework to assess the risk of slope failure. Two models are developed. The first was a local model that assesses

probabilistic factors of safety for slope failure at each sample location and a regional model that assesses factors of safety for slope failure for each region.

The local model uses a first-order, second moment (FOSM) method with a Taylor series approximation of the factor of safety function to estimate factors of safety within an assumed lognormal distribution for factor of safety. Variance is considered within \pm one standard deviation of the mean for estimating partial derivatives of the function. Results of the local model are presented as a percentile chart which is used to compare the factors of safety distribution for the sampled sites. The results indicate that at the sample sites, the Orphan study region is least likely to have a factor of safety less than unity, followed by the Scotian slope and St. Pierre slope study regions respectively.

The local probabilistic model was also used to assess the impact of using less conservative estimates for factor of safety. With the lognormal distribution assumption for factor of safety, estimates for 50, 75 and 90 percentile values of factor of safety are computed. The higher percentile values result in more conservative assessments of slope stability and a greater likelihood of a factor of safety less than unity. Generally, for the 90 percentile factor of safety, the likelihood of a factor of safety less than unity is approximately 3%, 10%, and 18% for the Orphan Basin, Scotian slope and St. Pierre slope study areas, respectively.

Finally, the local probabilistic model was used to assess reliability of the analysis method by calculating the reliability index at depth for each sample site. The results indicate that the Orphan Basin has the highest reliability followed by Scotian slope and St. Pierre slope with average reliability index values of 19.7, 7.1 and 3.8, respectively.

The reliability index corresponding to the estimated factor of safety for each sample site was plotted for all three study regions. The results reveal that if reliability index is the governing criteria for offshore slope stability assessment, a factor of safety of unity is inadequate to achieve the degree of risk desired. The variability of the data indicates that a factor of safety of 5 as a lower threshold is more appropriate for the method used (i.e., infinite slope method using undrained shear strength in a total stress model).

6 CONCLUSIONS

The objective was to conduct a comparative geohazard assessment of slope stability for the Scotia slope, St. Pierre slope and Orphan Basin. This project reviewed geotechnical data from 127 cores collected on 17 cruises. The slope stability was assessed using both deterministic and probabilistic methods. Generally, the probabilistic methods produces similar results to the deterministic method but offers greater understanding of what is measured and the reliability of the measurement. Additional conclusions are presented below.

1. The Orphan Basin is the most stable region, followed by the Scotian slope and St. Pierre slope regions. The difference in stability is generally related to differences in seabed inclination.

2. In order to meet general acceptable criteria for reliable performance the lower bound factor of safety criteria for assessment of slope stability should be 5, not unity (when using the infinite slope method for a total stress analysis).

3. The probabilistic analysis provides a more complete assessment of risk and reliability of analysis of factor of safety. Reliability of the assessment is assessed and can be compared with target reliability. If the relative reliability needs to be improved, variation of the variance interval can be used and new factors of safety calculated, all within the same dataset.

4. The current engineering model only considers the static load case for the study area. Further consideration of loading and other possible load combinations is required to fully understand geohazards in the study area.

ACKNOWLEDGEMENTS

The authors express their gratitude to the officers, crew, and scientific staff of the CCGS Hudson for their efforts in the field, particularly during cruises 1999-036, 2000-036, 2000-042, 2002-024, 2002-046, 2004-030, 2005-033 and 2006-048. The Geological Survey of Canada and the Canadian Program for Energy Research and Development funded this research. The authors thank Kate Jarrett for processing many of the cores and Gordon Fenton who provided insight and critical review.

REFERENCES

- Clarke, J.E.H. 1990. Late stage slope failure in the wake of the 1929 Grand Banks earthquake, *Geo-Marine Letters*, 10: 69-79.
- Meyerhof, G.G. 1985. Development of Geotechnical Limit State Design, *Canadian Geotechnical Journal*, 32: 128-136.
- MECO. 2007. Slope stability of central Scotian shelf. *MECO Report 5010*.
- Mosher, D.C. and Piper, D.J.W. 2007. Analysis of multibeam seafloor imagery of the Laurentian Fan and the 1929 Grand Banks landslide area, *Submarine Mass Movements and Their Consequences, III*, Springer, The Netherlands, 77-88.
- Mosher, D.C., K.Moran, and R.N. Hiscott. 1994. Late Quaternary Sediment, Sediment Mass Flow Processes and Slope Stability on the Scotian Slope, Canada, *Sedimentology*, 41: 1039-1061.
- Piper, D.J.W., Shor, A.N., Farre, J.A., O'Connell, S. and Jacobi, R. 1985. Sediment slides and turbidity currents on the Laurentian Fan: Sidscan sonar investigations near the epicentre of the 1929 Grand Banks earthquake, *Geology*, 13: 538-541.

- Piper, D.J.W., and Normark, W.R. 1982. Acoustic interpretation of Quaternary sedimentation and erosion on the channeled Upper Laurentian Fan, Atlantic margin of Canada, *Canadian Journal of Earth Sciences*, 19: 1974–1984.
- Tripsanas, E.K., Piper, D.J.W. and Jarrett, K.A. 2007. Log of piston cores and interpreted ultra-high-resolution seismic profiles, Orphan Basin, *Geological Survey of Canada Open File 5299*.
- Wade, J.A., and MacLean, B.C. 1990. The geology of the southeastern margin of Canada, *Geology of the continental margin of eastern Canada, Geology of Canada*, Ottawa, 2: 167-238.